

1
2
3
4
5
6
7
8
9
10
11
12
13
14
15
16
17
18
19
20
21
22
23
24
25
26
27
28
29
30
31
32
33
34
35
36
37
38
39

SOILS, SEC # • RESEARCH ARTICLE

Sediment provenance, soil development, and carbon content in fluvial and manmade terraces at Koiliaris River Critical Zone Observatory

Daniel Moraetis • Nikolaos V. Paranychianakis • Nikolaos P. Nikolaidis • Steve A. Banwart • Svetla Rousseva • Milena Kercheva • Martin Nenov • Toma Shishkov • Peter de Ruiter • Jaap Bloem • Winfried E. H. Blum • Georg J. Lair • Pauline van Gaans • Marc Verheul

D. Moraetis (✉)

Sultan Qaboos University, College of Science, Earth Science Department

e-mail: moraetis@mred.tuc.gr

N. V. Paranychianakis • N. P. Nikolaidis

Technical University of Crete, School of Environmental Engineering

S.A. Banwart

The University of Sheffield, United Kingdom

S. Rousseva • M. Kercheva • M. Nenov • T. Shishkov

Institute of Soil Science, Agrotechnology and Plant Protection "N. Poushkarov"

P. de Ruiter • J. Bloem

Wageningen University, Netherlands

W. E. H. Blum • G. J. Lair

University of Natural Resources and Life Sciences, Austria

P. van Gaans • M. Verheul

Deltares Soil and Groundwater System Soil and Urban Groundwater

(✉) **Corresponding author:**

Moraetis Daniel

Tel: +302821037786

e-mail: moraetis@mred.tuc.gr

40 **Abstract**

41 *Purpose* The purpose of this study was the investigation of sediment provenance and soil formation processes
42 within a Mediterranean watershed (Koiliaris CZO in Greece) with particular emphasis on natural and manmade
43 terraces. Koiliaris CZO is characterised by steep slopes, abrupt climatic changes, complex geology and most
44 importantly by a significant anthropogenic influence.

45 *Material and methods* Five sites (K1-K5) were excavated and analysed for their pedology (profile description),
46 geochemistry (including Rare Earth Elements and other trace elements), texture and mineralogy along with
47 chronological analysis (optical luminescence dating). The selected sites have the common characteristic of being
48 flat terraces where soil formation has been taking place and erosion is low. The selected sites differed with
49 regard to bedrock lithology, elevation and land use. Soils were classified as, Fluvisol (K1-K2), Leptosol (K3)
50 and Cambisol (K4-K5).

51 *Results and discussion* Three characteristic processes of soil genesis were identified: i) sediments transportation
52 from outcrops of metamorphic rocks and sedimentation to fluvial sites (K1-K2), ii) in situ soil development in
53 terraces with metamorphic rocks as parent material (K3) and in terraces with limestone as parent material (K4),
54 and iii) strong eolian input and/or material transported through gravity from upslope at the mountainous site
55 (K5). Only two sites revealed pedogenic processes such as a) calcite deposition in the fluvial environment (K1)
56 which was a relict evidence of dry period and b) clay illuviation and REE horizonization at site K4 which
57 corresponded to wetter period in Greece (medieval warm period). The REE patterns revealed strong
58 characteristics inherited from the bedrock at sites K4 and K5, while MREE and HREE depletion were observed
59 at K1, K2 and K3 sites. Carbon sequestration throughout the soil profile was high at manmade terraces at higher
60 elevation compared to fluvial environments due to both climatic effects and possibly intensive anthropogenic
61 impact.

62 *Conclusions* Soils at Koiliaris CZO are rather new soils with limited evolution. Pedogenic processes were
63 identified in the older sites like K1 site. The manmade terraces at higher elevation have much higher carbon
64 sequestration compared to the anthropogenic impacted fluvial areas. The intense agriculture activities have
65 discernible impact in the upper soil horizon even at higher elevation sites like the site K3.

66

67 **Keywords** Carbon content • Land use • Mediterranean watershed • soil development

68

69

70 **1 Introduction**

71 Soil loss rates typically exceed by far the rates of formation as a consequence of unsustainable land use practices
72 (Anderson et al. 2008; Brantley et al. 2007). Humanity has already degraded or eroded more than one third of all
73 arable land and continues to lose farmland at a rate of 0.5% a year — yet expect to feed more than 9 billion
74 people by 2050 (Montgomery 2010). The crucial role of soil functions and services has been acknowledged as a
75 precondition of meeting Millennium Development Goals related to elimination of poverty and hunger (MEA
76 2005).

77 Understanding the factors regulating soil formation processes and losses is of paramount importance to predict
78 the evolution of soils in the long-term under different climatic and/or management scenarios. This importance is
79 emphasized by the development of currently seventeen Critical Zone Observatories around the world (Banwart
80 2011) and individual studies dealing with soil development and soil functions (Eger et al. 2011; Solleiro-
81 Rebolledo et al. 2011; Scarciglia et al. 2011). These studies have improved our understanding on the factors
82 regulating pedogenesis including, landscape setting, climate, biota, human activities and their interactive and/or
83 synergistic effects. In addition, current methodological improvements and technological advances have boosted
84 our capabilities for elucidating pedogenic processes. Technological advances in rare earth element (REE) and
85 trace element analysis in soils with ICP-MS, promoted the identification of redox fronts and weathering
86 processes respectively (Laveuf et al. 2012; Laveuf et al. 2008; Long-Jiang et al. 2009; Zhaoliang et al. 2006).
87 These processes can be projected on a historical time series with the use of optically stimulated luminescence
88 dating (OSL) as it has already been used in sediments landscape evolution, geoaerology (Pope et al. 2008;
89 Zacharias et al. 2009) and pedogenic processes (Lair et al. 2009)..

90 Such information becomes even more critical in regions like the Mediterranean where the complex lithology,
91 geology and geomorphology of the landscape, and the intense climatic gradients set a unique and challenging
92 environment for tracing soil evolution. In such landscapes, soils often have evolved under the action of strong
93 winds and storms, at steep slopes and intense human activities which render them particularly fragile and
94 vulnerable to degradation and desertification (Barea et al. 2005). Mediterranean shrublands have been suggested
95 to currently be reaching “tipping” points which means an abrupt change from one stable state to another e.g. no
96 desertification to desertification (Kéfi et al. 2007). Likewise, the abandoned terraces in the mountainous areas of
97 western Crete, underlain by hard rock (limestones, phyllites-quartzites), have been identified as high erosion risk
98 areas (Grove and Rackham 1993, Arianostou 2001). Dotterweich (2013) presented a global perspective on the
99 fact that soil erosion was influenced by factors like natural setting, agriculture practices and socioeconomic
100 conditions. Moreover, the intensive agricultural practices adopted in the fluvial areas since the Neolithic period
101 (and mostly during Minoan period) may have adversely influenced critical soil functions associated with fertility,
102 productivity and carbon sequestration. Overgrazing, a common situation in the hilly and mountainous
103 Mediterranean landscapes (Stamati et al. 2011), further accelerates land degradation by decreasing plant cover
104 and intensifying rainfall-induced erosion. The most critical impact on soil evolution, however, arises from direct
105 human activities, primarily the intensive tillage methods adopted throughout the Mediterranean basin (Casana
106 2008). While such practices and soil denudation might stimulate soil formation by increasing the surface area of
107 minerals and rocks exposed to weathering (Bayon et al. 2012; Raymond and Cole 2003), intensive land use
108 practices have been often associated with severe impacts on soil structure (Bronick and Lal 2005) and hence on

109 carbon sequestration (Six 2004a; Six et al. 2000a; Six et al. 2002) which appear to be dependent on prevailing
110 climatic conditions (Sarah 2005).

111 Clearly, the knowledgeable approach on accurate soil profile description corroborated by a time frame would be
112 vital to the preservation of soils in the Mediterranean basin. The understanding of the soil evolution under the
113 influence of intense human activities for millennia would offer a valuable case study for adapting appropriate
114 agricultural management practices. This is particularly important due to the growing demand for land use
115 intensification (UNEP 2012). Koiliaris watershed in Crete (Greece) extends over 130 km², with a rain gradient
116 ranged from 447 to 1075 mm on average and at least three different lithologies where the soils have developed
117 under various land uses (Kourgialas et al. 2010). Moreover, the landscape is shaped by steep upland slopes
118 (more than 60% of the area has gradient higher than 11 degrees), karstic systems (sink holes) and flat fluvial
119 environments. The areas, where erosion dynamics do not exceed pedogenic processes in Crete, are those in
120 fluvial natural terraces and manmade terraces. The main objective of this work is the investigation of abiotic
121 material origin in soil in natural and manmade terraces, and the description of pedogenesis processes within the
122 time frame set from OSL results. The combination of geochemical analysis (REE, trace elements, major
123 elements), mineralogical characterization, and physical characteristics were used for the identification of the
124 critical factors that have affected and regulated the current state of soils in Koiliaris CZO. The results of this
125 study can be extended to other Critical Zone Observatories that represent different stages of evolution and
126 degradation of soils (Banwart 2011).

127

128 **2 Material and Methods**

129 2.1 Geological, geomorphological and hydrological setting

130 The geology of Koiliaris CZO is comprised of Plattenkalk nappe, Trypali nappe, Phyllite-Quartzite nappe,
131 neogene sediments and alluvium sediments (**Fig. 1**). The Plattenkalk nappe is the autochthonous nappe in the
132 stratigraphy of Crete and successively all the other nappes are piled in the order described previously (Baumann
133 et al. 1976; Dornsiepen et al. 2001; Papanikolaou and Vassilakis 2010). Plattenkalk is a cherty limestone with
134 sparse intercalations of shales and silicious beds (30-40 cm). The Trypali nappe is composed of re-crystallized
135 limestones and dolomites. Neogene formations include marls and marly limestones. Phyllites and quartzites are
136 metamorphic rocks, comprised of quartz and micaceous minerals. The alluvium deposits are comprised of river
137 sediments such as conglomerates and sands. The geomorphology at Koiliaris CZO consists of low-lands with
138 very gentle slopes (< 5°) where mainly alluvium and neogene formations outcrop and cover 27% of Koiliaris
139 CZO; areas at 200-600 m elevation (slopes with gradient of 10-20°) where metamorphic rocks and allochthonous
140 Trypali limestones cover 47% of the watershed; and areas at 600-2000 m (slope gradient greater than 20°) where
141 the autochthonous Plattenkalk limestones and the allochthonous Trypali nappe outcrop and covering the remaining
142 26% of Koiliaris CZO. Overall, the area with slope gradient between 0-5°, 5-17° and >17° covers 20%, 33% and
143 46% of Koiliaris watershed, respectively.

144 The hydrologic characteristics at Koiliaris CZO are related to geomorphological and lithological features. The
145 karstic system drains the rain and the snow melt in deep karstic aquifers which outflow in springs (Stylos spring
146 in **Fig. 1**) in low elevation in the boundaries of the fluvial environment with higher elevation land. Milavlakas (2)
147 and Mantamas (3) tributaries are mainly karstic areas and flow is rather sparse (**Fig. 1**). Eleven flood events
148 occurred in the period from 2004 to 2008 (Moraetis et al. 2010) which corresponded to flood events from the

149 area where metamorphic rocks outcrop in the watershed. Specifically, Keramianos tributary (1)
150 which drains a sub-basins comprised of metamorphic rocks have been found to transport large amounts of
151 sediments (Kourgialas et al. 2011) and deposits them in the fluvial areas of the watershed.

152

153 2.2 Site selection

154 Five sites (K1-K5) were selected for intensive soil profile characterization (**Fig. 1S** and **Fig. 2S** in the
155 supplementary information with profile photos). The criteria fulfilled in all sites included low slope gradient
156 ($<5^\circ$) which means areas where soil development was not constrained by erosion (gray shaded areas in **Fig. 1S**).
157 Crete has been tectonically active since late Eocene and steep slopes ($>11^\circ$) cover 61% of the watershed, spread
158 especially at elevations higher than 300 m (white areas in **Fig. 1S**). On the other hand low gradients ($<5^\circ$) (**Fig.**
159 **1S**) occur in fluvial areas and in some manmade terraces.

160 Manmade terraces have been extensively constructed mainly in steep slopes at elevations >300 m during
161 Venetian (1211–1669 AD) and Ottoman period (1669–1898 AD), to increase arable land (Stallsmith 2007). It
162 was generally believed that terraces have been adopted since Hellenistic and Roman period (or earlier) in Crete,
163 however no detailed studies exist regarding the landscape evolution history of western Crete.

164 Bedrock lithological variability in the sampling areas includes limestones, metamorphic rocks and alluvium
165 sediments. Vegetables, olive trees (tilled in fluvial environment and terraces), old olive trees in manmade
166 terraces (non affected by tillage) and abandoned manmade terraces (pasture lands) are among the common land
167 uses in the island of Crete and were included in our site selection. All sites exhibited slopes with gradient of less
168 than 5° . **Fig. 2** summarizes the geomorphology, the bedrock and current land use for all sites along with the
169 profile characterization as described later.

170 **K1-K2 sites:** The soil at K1 and K2 sites developed in alluvium sediments; they are intensively tilled, and
171 cultivated with vegetable crops and olive trees, respectively. The average annual rainfall and temperature is 567
172 mm and 21° C, respectively. The area at K1 and K2 sites is considered as non-active floodplain.

173 **K3 site:** Soil at K3 site situated on manmade terraces with metamorphic rocks (phyllites-quartzites). Terraces
174 have been cultivated with olive trees subjected to annual tillage. The olive trees were of approximately the same
175 age as at K2 site (~ 20 years). The average annual rainfall and temperature are 969 mm and 18° C, respectively.

176 **K4-K5 sites:** Soils at K4 and K5 have been developed onto platy and cherty limestones. Land use at K4 is
177 terraces with non-tilled olive trees (~ 50 years old) and abandoned terraces dominated by shrubs and subjected to
178 grazing at K5 (red dashed lines in Fig. 1S in supplementary information). At K4 site, the average annual rainfall
179 is 915 mm and the average temperature is 18° C, while at K5 site is 1335 mm and 14° C, respectively.

180

181 2.3 Sampling, profile characterization and analytical techniques

182 Three soil pits, for each of the selected sites (K1-K5), were excavated. For each of the five sites one pit was
183 assigned as the “main” soil pit while the other two were assigned as the “secondary” pits. The criteria for the
184 “main” soil pit selection were low disturbance (e.g. erosion, fire, sedimentation) and low stony intercalations.
185 The soil profiles from the “main” soil pits were sampled and analyzed in all identified horizons while the
186 “secondary” profiles were selectively sampled to assess spatial variability.

187 Chemical (bulk chemistry, trace elements and REEs) and mineralogical analyses (for fraction <2mm and <2µm)
188 were performed on the different horizons of the main soil profile at each site. Table S1 provides an overview of
189 these analyses, while gray bands in **Fig. 2** depict the sampled horizons in soil profiles.

190 Bulk chemical analysis was performed using a x-ray fluorescence energy dispersive spectroscopy (XRF-EDS)
191 (S2 Ranger, Bruker EDS) on the soil fractions <2mm and <2µm with fusion beads. XRF-EDS was also
192 employed for the analysis of Zr and Nb. Trace elements (Li, B, Ti, Cr, Mn, Ni, Cu, Zn, As, Rb, Sr, Y, Cs, Ba, Pb,
193 U) and REE content was assessed by inductively coupled plasma mass spectrometry (ICP-MS) following the
194 methodology developed by Marini et al. (2005) with the inclusion of a pre-treatment stage for carbonate
195 removal. Digestion included the following steps: a) initial dissolution with HCl until dryness; b) dilution with HNO₃;
196 c) dissolution with a mixture of HF, HNO₃, and HCl; d) addition of EDTA and microwave digestion; e) dryness and
197 dilution with HNO₃. REEs were normalized to shale composite (NASC) REE content (Gromet et al. 1984). In
198 addition, Ce anomaly was calculated following the equation $(3 \times Ce/Ce_{shale}) / [(2 \times La/La_{shale}) + (Nd/Nd_{shale})]$ given by
199 Elderfield and Greaves (1982).

200 Mineralogical analysis was performed with a D8 Advance (Bruker) X-ray diffractometer and 2θ running from 4
201 to 70° with 0.019° step (Anode: Cu 1.54 Å, 35 kV, 35 mA). All analyses were performed with addition of an
202 internal standard (corundum ~15% w/w). Qualitative and quantitative data were derived using the SOCABIM
203 software (EVA, TOPAS). Additional mineralogical analyses included estimation of kaolinite content after
204 heating at 550 °C for 2 h, and montmorillonite content after leaving the samples in glycol for 16 h at 60° C.

205 Carbon content (C), carbonate content (CaCO₃), particle size distribution (PSD), pH and electrical conductivity
206 (EC) were also assessed in all the horizons. Electrical conductivity and pH were measured at a soil:water ratio of
207 1:2.5 (Soil survey staff, USDA 2004). Carbonate content was measured with 10% HCl acid and the evolved
208 carbon dioxide (CO₂) quantification (Soil survey staff, USDA 2004). For verification some samples were also
209 measured after dry combustion with prior removal of organic carbon through heating at 550 °C (Soil survey staff,
210 USDA 2004). Bulk density was measured in the horizons where gravels and roots were limited, by using ring
211 tubes with length of 5 cm.

212 Soil PSD was obtained after dispersion of the sample with sodium hexametaphosphate (NaPO₃)₆ without
213 removal of organic matter and carbonates from the soil sample. Sand fraction was separated by sieving, and the
214 particle fractions < 0.05, <0.02, <0.01, <0.002 mm were determined by pipette method. Finally total organic
215 carbon (TOC) was measured with a Carlo Erba Analyser 1500.

216 Samples were collected for optical stimulated luminescence (OSL) dating using plastic tubes (6 cm in diameter and
217 20 cm in length). OSL sampling was not performed in K3 and K4 sites since they were thin and gravelly
218 respectively. The OSL sampling depth was at 0.85, 0.45 and 0.45 cm at K1, K2 and K5 sites, respectively. Thus,
219 samples from three pits were dated by OSL for the quartz coarse grain fraction in the University of Natural
220 Resources and Life Sciences in Vienna. Quartz extracts were checked for feldspar contamination using infrared
221 stimulation. Blue light-emitting diodes (LEDs) were used for the optical stimulation of quartz for 40 s at 125°C
222 (Lomax et al, 2012).

223

224 2.4 Quality control and statistical analysis

225 PSD, SOM, calcite content, pH and EC were measured for both the main and the secondary profiles thus;
226 average values and relative standard deviation (RSD) are presented (Table 1) so as to show spatial variability in

227 each site. Some of the chemical analyses were performed for the main pit in triplicates for assessing
228 measurement quality. Specifically, for trace elements, in addition to routine double runs of the same sample,
229 triplicate samples were analyzed to assess precision, calculated also as relative standard deviation (RSD). The
230 same procedure was followed for REEs, whereas additionally spiked samples and the international standard
231 hornblendite (JH-1) were analyzed to assess trueness (Imai et al. 1998). The quality control results are presented
232 in Tables S2 and S3 (supplementary information). The error in JH-1 standard measurement ranged from 2-13%,
233 whereas triplicates and double run of the same sample exhibited relative standard deviation 1-9%. The REE
234 spike recovery ranged from 85 to 93%. The error in the trace element triplicate measurements and the double
235 runs in the same sample exhibited relative standard deviations of 3-15% and 0.2-12% respectively. Finally, the
236 error associated with the mineralogical quantitative analysis was on average 11%.

237

238 **3 Results**

239 3.1 Profile characterization

240 The presentation of results for bulk chemical and physical characteristics is organized in groups according to
241 bedrock material. Thus, K1 and K2 were classified in the first group (fluvial sediments), K3 in the second
242 (metamorphic rock) and K4 with K5 in the third group (Plattenkalk limestones). K1 and K2 soils were
243 characterized as Calcic Endogleyic Fluvisol and Calcic Fluvisol respectively (FAO 2006). The profiles sampled
244 at the Koiliaris CZO alluvial fan had depths 100 and 72 cm for K1 and K2, respectively. Pedological
245 observations at K1 and K2 sites revealed that they were tilled, and only AC and C horizons were identified in
246 both soils. Calcite content was higher for the K1 site compared to K2 site. Munsell color (dry) was 10YR 6/4
247 (light yellowish brown) and 7.5YR 6/6 (reddish yellow) for K1 and K2 sites respectively and the pedality was
248 described as weakly coherent and loose for both sites. Ceramic debris was found at site K1 at a depth of 90 cm.
249 The soil profile at K3 site was the thinnest (36 cm) which was disturbed by tilling and it was classified as Haplic
250 Leptosol (FAO 2006). ACp and CR horizons were identified in the soil profile at K3. Low concentration of
251 calcite was identified and the Munsell color (dry) was 7.5YR 6/6 (reddish yellow) with a moderate pedality with
252 loose consistency. K4 and K5 soils were classified as Endoleptic and Bathyleptic Cambisol (FAO 2006)
253 respectively and they have developed Ah and AC horizons. The soil of site K4 was relatively shallow (60 cm),
254 whereas that of K5 extended much deeper (90 cm). The Munsell color (dry) was 5YR 5/6 (yellowish red) for K4
255 and 7.5YR 5/4 (brown) for K5. Pedality was strong for the K4 site and moderate for K5 site. No tilling was
256 identified at either site.

257

258 3.2 Chemical and Physical analyses

259 The chemical and physical characteristics of the different soil horizons as well as the XRF chemical analyses of
260 the 2 mm soil fraction in all sites are summarized in Tables 1 and 2. The Si/Al ratio (hereafter we referred to
261 elemental ratio) is lower at K1 site (~4) compared to K2 (~5.5) while the soil at the former site is mainly silty-
262 loam and at K2 is sandy-loam (**Fig. 3S**: supplementary information). TOC content ranged from 15 to 2.9 g/kg in
263 the K1 profile and from 19 to 4.9 g/kg in the K2 profile. K1 has higher bulk density (1.47 g/cm^3) in all horizons
264 compared to K2 (1.24 g/cm^3). The pH of site K1 ranged from 7.7 in the upper horizons to 8.1 in the lower
265 horizons in accordance with increase in calcite content (mineralogy is presented below) and decrease in organic
266 content. Lower pH values, ranging from 6.5 to 6.9 were measured at K2 site which were consistent with the

267 lower CaCO₃ content and the higher organic carbon compared to K1 site (Table 1). The Na₂O and MgO content
268 at K1 and K2 sites was comparable to this at K3 site and much higher compared to the other sites. The CaO
269 content at both sites was higher compared to the other sites. Higher EC values were measured at site K1 (317-
270 296 μS/cm) than at site K2 (150-93 μS/cm). K3 site has a Si/Al ratio of approximately 2.6 for both the AC and
271 CR horizons and it was classified as sandy-loam (**Fig. 3S**: supplementary information). The pH ranged from 6 in
272 the ACp to 7.4 in the CR horizon, an effect attributed to the higher calcite content in horizon CR while low
273 values of EC were assessed (93-58 μS/cm). The CR horizon at K3 site has a higher TOC (18 g/kg) compared to
274 ACp (15 g/kg) and bulk density was 1.38 g/cm³ and 1.27. g/cm³ respectively. The K₂O content at K3 site was
275 higher compared to K1, K2, and K4 site but lower than that at K5 site. The MgO content in soil at K3 was in
276 between the values in soils at K4 and K5, while Na₂O content was higher in soil at K3 compared to soils in both
277 K4 and K5 sites.

278 Despite their presumably common parent material, the soils at K4 and K5 diverged greatly. The K4 soil profile
279 had a Si/Al ratio of 7.8 for the Ah and 6 for the AC horizon, whereas these values were 2.3 and 2.6 respectively
280 for K5 site. The texture at K4 and K5 sites are silty-clay-loam and silty-clay respectively (**Fig. 3S**:
281 supplementary information). The pH ranged from 5.7 to 4.7 in the profile at K4 site and it was around 6, with no
282 downward variation, at site K5. Both sites were characterized by low calcite content. The EC ranged from 167
283 to 73 μS/cm at site K4 and 96 to 75 μS/cm at site K5. The TOC decreased from 72 g/kg in the upper horizon to
284 5 g/kg in the lowest one at K4 site and from 42 to 16 g/kg at K5 site. Bulk density ranged from 1.10 at site K4
285 for Ah horizon and 1.06 to 1.21 at K5 site for Ah and Ac horizon, respectively. Bulk density data were not
286 obtained at K4 site due to high stone content. Contents of K₂O and MgO at site K5 were 2-4 times higher than
287 those at site K4 and overall higher than those to the other sites.

288 The chemical analysis of the clay fraction for the different soil horizons is presented in Table 3. Na₂O was not
289 measured since the dilution factor in the fusion beads (XRF-analysis) was high. MgO was higher at site K5. The
290 Si/Al ratio did not differ among sites (~1.8) apart the higher ratio at the C2k horizon at site K2 (2.8) and the
291 lower ratio at site K3 (1.5). Loss of ignition (LOI) in the clay fraction indicates the break down of carbonates,
292 loss of mineral-structural water and degradation of organic compounds. K2 site has the highest percentage of
293 LOI (25, 29, and 26%), whereas K4 and K5 showed relatively low LOI values (~20%).

294 Two principal component analyses (PCA) were performed; the first PC was fed with the texture results (silt,
295 clay, sand), calcite content, pH and TOC and the second with the trace element contents. The first PCA
296 classified soils into three groups (**Fig. 3a**): K4 and K5 sites comprise the first group (red dashed line **Fig. 3a**),
297 K2 and K3 the second group (black dashed line **Fig. 3a**) and K1 the third group. The derived clustering showed
298 that clay, silt and TOC were the most critical factors for classifying soils of K4 and K5 sites, sand was the
299 critical factor for grouping K2 and K3 sites and finally calcite and silt content were the influential properties in
300 K1 site (bi-plot in **Fig. 4Sa, b**: supplementary information). The factors described previously were related to
301 textural differences and calcite content in the sites. The second PC analysis showed a slightly different
302 clustering of the investigated sites. Three contrasting patterns were observed, the separation of K4 and K5 sites
303 into different groups and the categorization of K1, K2, K3 sites into one group (blue dashed line **Fig. 3b**). The
304 second PC analysis showed that the K5 site exhibited correlation in Mn, Ni, Cr, Fe, while K4 site in U, As, Y,
305 Li, Ti. Sites K1, K2 and K3 ascribed to the third group and exhibited higher content of Zr and Nb compared to
306 the other sites. The clustering of the second PCA gives important information on the geochemistry of soils

307 which was attributed to the parent material origin (bi-plot in **Fig. 4Sa, b**: supplementary information).
308 Specifically, K1, K2 and K3 sites showed common origin of their parent material and that was evident also in
309 the mineralogical analysis as it is presented below. Site K4 showed Ti, Y and Li interrelation which is related to
310 the more acidic chert intercalations (**Fig. 5S and Table S4**: supplementary information). In contrast, site K5 has
311 the highest trace element content specifically for Ni and Cr whereas elements such as Fe, Mg and Mn also
312 occurred in high concentrations (**Table 2, Table S5** in supplementary information).

313

314 3.3 Mineralogical analysis

315 Mineralogical analysis was conducted on the <2mm and <2 μ m soil fractions (Table 4). The average content of
316 quartz in the <2mm fraction for the upper two soil horizons was 52, 53, 44, 48, and 24 % for K1, K2, K3, K4,
317 and K5 respectively. Soils at sites K1, K2 and K3 contained paragonite which was interpreted as being a
318 primary mineral from the metamorphic rock like the bedrock at K3 site. Soils at K1 and K2 sites contain zeolite
319 (phillipsite) which is commonly met in fluvial environments having undergone the influence of alkaline waters
320 like those flowing from karstic springs (e.g. Stylos spring) of Koiliaris CZO. A higher illite content in the <2mm
321 soil fraction was identified at K5 (28-41%) compared to K4 site (17-27%). By contrast K1, K2 and K3 sites
322 showed the lowest illite content (1-4%) at the same fraction. Calcite content was identified at K1 and K2 site
323 and it was absent from the other sites. K4 site exhibits high quartz content which was linked to the chert
324 intercalations in the bedrock (**Fig. 5S** in supplementary information). In contrast, K5 site showed much lower
325 quartz content compared to K4 site suggesting that K5 site has different geochemical characteristics despite the
326 common bedrock of both sites (**Table S4**: supplementary information). Kaolinite was higher at K4 site (19-23 %)
327 in the fraction <2mm compared to the other sites (K1:9.2, K2:9.5, K3:11.5, K5:13.8 on average) whereas K5 has
328 a significantly lower kaolinite content (11-14%). Chlorite was clearly identified after the heating test only in the
329 K5 soil, while very low content of vermiculite was identified in the K1, K2 and K3 soils

330 The <2 μ m fraction exhibited mainly secondary minerals such as illite, kaolinite, muscovite and some oxides
331 (Table 4). Primary minerals, quartz and paragonite were found in the clay fraction of K1, K2, and K3 sites.
332 Calcite was identified in the clay fraction at K1 site whereas it was absent from K2 site. The most abundant
333 mineral in the clay fraction at all sites was illite, ranging from 29% (K3) to 48% (K5). Kaolinite content ranged
334 successively from lower (14%) to higher values (37%) according to the order K5, K1, K2, K3, K4 sites.
335 Muscovite can be also considered as primary mineral originating from the metamorphic rocks and Plattenkalk
336 limestones.

337

338 3.5 OSL soil dating

339 OSL dating was performed at sites K1, K2 and K5 (Table 1). The dating at K1 site exhibited the age of 2400
340 (\pm 400) year in 0.85 m depth and that could suggest that the ceramic debris identified was probably of the
341 Hellenistic period. The age of the soil at the K2 site was estimated to be 1400 (\pm 400) years old at the depth of
342 0.45 m. On the other hand K5 site consisted of much younger soil (580 years \pm 120) and that could correspond to
343 Venetian period when the construction of terraces was a very common practice. Overall the ages estimated by
344 OSL were no older than late Holocene.

345

346 3.6 REE analysis

347 The average total REE content of the upper two horizons was 144, 119, 173, 267, and 205 mg/kg for K1, K2,
348 K3, K4, and K5 sites, respectively. The total REE content increased downward at K1, K2, and K3 sites by 8, 4,
349 14 %, respectively, while a greater increase of 67% and 17% was found for K4 and K5 respectively. The
350 following observations can be made regarding the shape of the REE pattern, the Ce anomaly and the
351 horizonization of the REE content:

- 352 • Shape of REE pattern - The ratio LREE/HREE[†] was calculated from the normalized to shale ratio of
353 La/Yb. The sites can be separated into two major categories, those with a high LREE/HREE ratio (**Fig.**
354 **4a**) and those with a low LREE/HREE (**Fig. 4b**). The soils at K1, K2, and K3 sites with LREE/HREE
355 values of 2.4, 3.3, and 4.4 respectively were classified in the first category while K4 and K5 sites in
356 the second category with values of 0.9 and 1.4 respectively.
- 357 • Ce anomaly - Values higher than 1 depict a positive anomaly, while lower than 1 a negative anomaly.
358 A Ce positive anomaly was identified for the sites K1 (1.13), K2 (1.14), and K3 (1.50) and a negative
359 anomaly for the sites K4 (0.66 to 0.62) and K5 (0.93 to 0.87) (**Fig. 4a** and **4b**).
- 360 • Horizonization of REE content - Another striking feature was the horizonization of REEs content
361 observed at site K4 (**Fig. 4b**: gray double arrow). Increase of 39% in the AC horizon (**Fig. 6Sa**:
362 supplementary information) and 67% in the C2 horizon (50-60 cm) was identified compared to the
363 REE content of the upper horizon (Ah) in K4 site. On the other hand, REE increase was only 17% at
364 K5 site (**Fig. 6Sb**: supplementary information). The total REEs content increase in lower horizons of
365 the other soil profiles at K1, K2, K3 was 8, 4, 14% respectively.

366 The REE pattern of the bedrock was also analyzed (**Fig. 4a** and **4b**). An Eu peak at the normalized REE (to
367 NASC-shale) concentrations, was identified for the metamorphic rocks (phyllite-quartzite) and to lower extent
368 for the limestones of the Plattenkalk nappe (K4 and K5). The Eu peak is usually associated with metamorphic
369 rocks or rocks which formed through diagenesis as it was the case for the Plattenkalk limestones (McLennan
370 1989). No Eu peak was identified in any of the soils. The negative Ce anomaly in the bedrock has been related
371 to the marine origin of the limestone deposits in the Plattenkalk nappe (Sholkovitz and Schneider 1991;
372 Johannesson et al. 2000; Mouslopoulou et al. 2011).

373

374 **4 Discussion**

375 4.1 Geochemical and mineralogical evidences of sediment provenance in soils at Koiliaris CZO

376 4.1.2 Natural non active river terraces at K1 and K2 sites

377 The mineralogy analysis showed that both soils had paragonite which was also identified at K3 site. The PCA
378 from the trace elements suggested that soils at sites K1, K2, K3 have similar geochemical characteristics. This
379 was also confirmed by REEs pattern for these sites (**Fig. 4a**). Indeed the area enclosed in the black dashed line
380 in **Fig. 1S** is covered by metamorphic rocks and more than the 50% of the area is dominated by slopes greater
381 than 11 degrees. The high relief and the brittle texture of the metamorphic rocks probably facilitated the erosion
382 especially under intensive cultivation. Thus the transport of sediments through Keramianos river (Tributary 1;
383 **Fig. 1**) towards the fluvial environment of Koiliaris River probably contributed significantly with eroded

[†] HREE: Ho, Er, Yb, Lu.
MREE::Eu, Gd, Tb, Dy
LREE: La, Ce, Pr, Nd, Sm.

384 material the fluvial terraces at K1 and K2 sites. The textural differences between K1 and K2 were expected in a
385 depositional environment due to different hydrodynamic conditions during sedimentation.

386 The same lithology at sites K1, K2 and K3 is also confirmed by the similarity of REE normalized patterns
387 (Compton et al. 2003; Xing and Dudas 1993). Soils at sites K1 and K2 developed on the weathered relicts
388 mainly of the metamorphic rocks transported from areas lithologically identical to site K3. Thus, the higher
389 Si/Al ratio in soil chemical analysis at K1 and K2 sites compare to K3 site and the identical REE patterns
390 reflected the weathered relicts from which the two soils (at K1 and K2) derived. The higher content of HREE at
391 site K1 compared to K2 and K3 can be explained by the pedogenic calcite deposition (Laveuf and Cornu 2009)
392 which was identified in the <2 μ m fraction of the site K1. The calcite presence in the clay fraction at K1 and not
393 at K2 site reveals also a strong carbonation process (calcite precipitation) in the former. The aforementioned
394 results are supported also from the calcite analyzed through acid dissolution which showed clear calcite increase
395 in lower horizons.

396

397 *4.1.2 Manmade terraces at site K3*

398 K3 site exhibited common geochemical characteristics with the sites K1 and K2 as it has been already
399 mentioned. The soil was very thin with the CR horizon close to the surface (10 cm) which showed limited
400 pedogenic evolution. Soil disturbance induced by the tillage and it was very discernible (**Fig. 1S**). The K3 site
401 was one of the two sites where the soil parent material derived from the bedrock (metamorphic rock) and that
402 was reflected from the high paragonite content (12-35%). The more intense positive Ce anomaly at K3 site than
403 at K1 and K2 sites (**Fig. 4a**) could be attributed to the immobilisation of Ce⁴⁺ arising from its precipitation (as
404 cerianite: CeO₂) in an oxidized horizon and probably adsorbed on clay surfaces (e.g. goethite) and organic
405 matter (Compton et al. 2003; Leybourne and Johannesson 2008). The higher content of Fe at the K3 site could
406 be an indication of available electron scavenger (oxidizer) from Ce³⁺ during the weathering process and hence,
407 the rapid deposition of cerianite. In most cases, the Ce⁴⁺ positive anomaly was accompanied by MREE
408 enrichment due to scavenging by Fe/Mn-concretions (Laveuf et al. 2012, Laveuf and Cornu. 2009, Laveuf et al.
409 2008), which was not observed in our case. Considering the MREE depletion and the Ce⁴⁺ positive anomaly, we
410 inferred that a) Ce³⁺ was readily oxidized and precipitated by the action of different oxidant than by Fe/Mn-
411 concretions b) some primary silicate minerals at site K3 may exhibit higher retention of cerium which was
412 inherited also in the soil. Indeed, Leybourne and Johannesson (2008) mention several cases of Ce⁴⁺ enrichment
413 due to interaction with other phases like e.g. organic matter, while Laveuf et al. (2012), showed REE patterns
414 for silicate minerals in soil which had Ce⁴⁺ positive anomaly and pronounced MREE depletion. Since no
415 fractionation studies performed on REE distribution in soils, both previous explanations were possible. HREE
416 are the most mobile REE during weathering, especial at pH \geq 6 and in our case HREE depletion followed that
417 trend (Aubert et al., 2001, Ma et al., 2002, Miao et al. 2008). Summarizing, the MREE and HREE depletion in
418 soils at K3 site and also at K1 and K2 sites were readily induced in the time frame set for the soil development
419 which corresponded to relatively young soils (see section 4.2). The Ce⁴⁺ positive anomaly could be rather a fast
420 oxidation-precipitation event or an inherent characteristic from primary silicate minerals. Finally the remark
421 depletion of Eu concentration in the soil compare to bedrock at least for K3 site (**Fig. 4a**) could be related to
422 plagioclase weathering, a significant Eu host, which is weathered fast with concomitant Eu leaching (Compton

423 et al. 2003, Murray 1991b.). The partitioning of Eu in sediments (depletion) and in water (positive) has been
424 described extensively by Leybourne and Johannesson (2008).

425

426 *4.1.3 Manmade terraces at K4 and K5 sites in Plattenkalk limestones*

427 The K4 site exhibited different provenance of the parent material compared to K5 site. Field observations
428 support that the K4 site soil developed partly on material derived from bedrock weathering as it was shown in
429 **Fig. 5S** (supplementary information-photo was taken from the side of the terrace) where highly resistant to
430 dissolution chert layers were observed and extended in the soil profile. On the other hand some manmade earth
431 movement (plow) could explain the lack of B horizon at K4 site as discussed below. Soil development showed
432 to be different at site K4 since kaolinite was higher at site K4 compared to that of site K5 which was not
433 expected due to lower elevation (and hence, less rainfall). Thus, more extensive time in soil evolution at K4 site
434 was possibly the reason of the kaolinite increase. Furthermore, soil at K4 site showed negative Ce anomaly
435 similar to bedrock (**Fig. 4b**), which is an inherited characteristic of soils developed from limestone bedrock
436 (Laveuf and Cornu 2009; Laveuf et al. 2012; Thomas 1993).

437 The K5 site showed a weaker Ce anomaly which could be evidence of mixing with other parent material apart
438 the Plattenkalk limestones, or due to preferential retention of Ce as described at K3 site, however the first is
439 supported also from the mineralogical differences between the two sites (Table 4).. The higher concentration of
440 elements such as Mn, Ni, Cr and Fe, as it has been already mentioned at site K5 showed a mafic origin of the
441 soil parent minerals. However, there was no evidence of mafic rocks in the vicinity. The same effect could be
442 related to extensive soil weathering and subsequently the increase of weathering resistant elements (e.g. Cr, Ni).
443 Soil at K5 site was relatively young (as from OSL data) with limited in-situ weathering time, thus mass transfer
444 due gravity from steep upland could have re-mobilized some weathered soil towards the terraces at K5 site. The
445 dust deposition of mafic or ultramafic dust could be also a reason of the mafic “component” in the soil, since
446 mountains in Crete with the high relief (2km) were the first steep land interacting with the dust trajectory stream
447 arriving mainly from northern Africa (Muhs et al. 2010). In addition, the higher rainfall, the land roughness and
448 partial snow cover (highly karstified) at high elevation were enhancing dust accumulation (Nihlén et al. 1993,
449 Wu et al. 2010). Two possible sources of dust deposition were considered; the first source had more erratic
450 supply like past eruptions at Santorini volcano (Siart et al. 2010); the second source was Sahara desert which
451 had more continues supply through northward winds. Sahara dust has high illite content rich in LREE like Ce^{4+}
452 (Kalderon-Asel et al. 2009; Muhs et al., 2010) and that coincided with the high illite content acted as adsorbent
453 of LREE at site K5 (PCA results **Fig. 3b**) (Coppin et al. 2002; Wan and Liu, 2005). Finally, even we were not
454 able to distinguish between the steep upland material transport and/or dust input, both considered responsible for
455 the geochemical differences at site K5 such as the large different Si/Al ratio.

456 The profile investigation supports the different evolution of the soils at sites K4 and K5. The soil at site K4 had
457 an A horizon of 5 cm thickness similar to K5 soil, however the AC horizon of site K4 was 5 cm and of K5 was
458 85 cm. Moreover, the K5 site was characterized by the lack of C horizon and there is no evidence of transition
459 from bedrock to soil which can be explained by a) the rapid deposition of erosional material transported from
460 the steep upland next to the terraces and/or the high rate of eolian material deposition, as already mentioned or b)
461 the material was brought in by humans from adjacent areas during the construction of the terraces.

462 At this point we analyzed the OSL results confidence in relation to parent material origin at K5 site. In the case
463 of eolian transport, quartz grains would have been bleached completely (clock was zeroed), whereas in the case
464 of material brought in by people some residual clock measuring may be included in the quartz grains. The
465 estimation of such discrepancy is related to OSL scattering estimation in a single sample (Davidovich et al.
466 2012). Such scattering was low in our case thus the OSL dating at site K5 was considered reliable and supports
467 mostly the eolian origin of the material and/or the possible mass transfer by gravity from steep upland. The
468 dating fits with the Venetian-Ottoman period when agricultural practices like manmade terraces in high
469 elevation were commonly employed to expand the cultivated area to support human needs and livestock
470 production. Identical terraces with stonewalls have been also identified in several Aegean islands (Kizos and
471 Koulouri, 2006, Charitopoulos and Sarris 2009).

472 Finally, clay illuviation was observed in the lower horizons of the K4 site, which was not evident for site K5,
473 suggesting that K4 has been evolved through the influence of wetter conditions compared to those prevailing at
474 site K5. Clay translocation in Mediterranean areas has been mainly reported during interglacial periods while in
475 present climatic conditions such profiles developed mainly in humid to sub-humid areas with good drainage
476 (Fedoroff 1997). The presence of B horizon at the K4 site was expected due to low pH and the clay illuviation
477 process but that was not observed. Hence, the lack of B horizon suggested the possibility of surface disturbance
478 at least with some plow event prior the non-tilling period after the olive trees plantation. Although it was not
479 possible to estimate the age of the soil at site K4 due to methodological constraints (rock and roots were present,
480 in addition the OSL method is not appropriate for soils with in situ development), the aforementioned evidences
481 support that the soil profile at site K4 developed under different climatic conditions (wetter conditions) than
482 those prevailing of site K5 and probably those of site K3.

483

484 4.2 Time frame in soil evolution and organic carbon content in terraces at Koiliaris CZO

485 Before setting the soil profiles under a timeframe according to OSL dating results it should be mentioned that a
486 B horizon was not identified in most of the sites sampled in the present work. The previous argument agreed
487 also with the pH values which are still under the carbonate-buffer ($\text{pH} > 6$) and the lack of illuvial clays, apart at
488 K4 site. This means a) that the soils have not gone through intensive weathering and leaching, Following the
489 oldest soil identified in the fluvial area (K1) it can be concluded that B horizon was not developed during Late
490 Holocene in western Crete.

491 The soil profiles and the findings of OSL dating were put into a time scale depicting the climatic variability for
492 the late Holocene as indicated from studies of sediments in two areas in Greece, in lake Dojran in northern
493 Greece (Francke et al. 2012) and Anapodaris river in Crete (Macklin et al. 2010 and references therein) (**Fig. 5**).
494 The calcite deposition at K1 site fitted perfectly with the arid period described in Dojran lake which was
495 characterized by decreasing sediment grain size and lower water level. After sediment deposition in the K1 site,
496 prolonged dry conditions (> 1000 years) could have stimulated the deposition of calcite. The prevalence of such
497 climatic conditions was also verified in sediment aggradation at Anapodaris river, which was characterized by
498 finer sediments from ca. 3 to 2 kyr BP (**Fig. 5**). The sediment at K2 site was deposited under more intense
499 hydrodynamic conditions compared to K1. Indeed, the OSL dating sets K2 site close to the wet period described
500 in the Djoran and Anapodaris river. The aforementioned period was named medieval warm period (MWP) (Le
501 Roy 1971) and it was characterized by humid and warm conditions (**Fig. 5**). The lower temperatures prevailed

502 between the 16th to 19th century following the MWP may have retarded calcite deposition as it has been also
503 described for Dojran lake (**Fig. 5**) (Francke et al., 2012). These shorter development time at K2 site compared to
504 K1 site could be considered responsible for the thinner AC horizon (15 cm at K2 site compared to 29 cm at K1
505 site), and the absence of an A horizon (**Fig. 2**).

506 The only manmade terrace in which soil age was estimated, was at K5 site and OSL dating revealed a recently
507 developed soil. The K5 site was developed during what was termed as “little ice age” with colder and arid
508 conditions (Wagner et al., 2009). The main characteristic for the site was a thick AC horizon, and the lack of
509 critical pedogenesis and the high organic matter content throughout the soil profile. K3 and K4 sites were not
510 dated; however the soil profile characteristics could give us an approximate timing, relatively to the other sites.
511 The soils at K3 and at K4 sites developed in situ and both terraces have been constructed to hold soil material.
512 The terrace construction at K3 site could have probably taken place at the same time as the widespread use of
513 terraces during Venetian (1211–1669 AC) and Ottoman period (1669–1898 AC) or later (dashed arrows with
514 question-marks in **Fig. 5**). The former is supported by the fact that no Minoan or Hellenistic settlements have
515 been identified in the vicinity of K3 site and the limited development of soil horizons. The K4 site exhibited
516 clay illuviation in the lower soil horizons which inferred that humid conditions have driven soil development
517 and evolution. The only wet period during the late Holocene was this described as warm medieval period
518 (WMP), thus, K4 site could be set tentatively in the time frame close to that period and prior to the development
519 of soil at K3 and K5 sites. However, A/AC horizons (20 cm) and C horizon (45 cm) thickness at K4 site is
520 similar to that of K1 site and the assumption of a younger soil compared to the soil of site K1 is not supported.
521 Thus, the soil at K4 site has been developed in situ and there is high probability to have been derived probably
522 earlier than the K1 soil. The climatic archives in Dojran lake and Anapodaris river showed highly wet periods
523 (not shown in **Fig. 5**) between 4,2-3 kyr and 5-3 kyr respectively and that may also be a candidate period for
524 development of soil in site K4 (dashed arrow with question-mark in **Fig. 5**). The previous hypothesis is
525 supported by a) the higher kaolinite content in both <2mm and <2 μ m fractions which means that leaching
526 processes lasted longer compared to the other sites b) the low soil pH denoting extensive weathering c) and the
527 clay illuviation. Thus, K4 site could be the older site compared to the others and clay illuviation was a relict
528 characteristic of a wet period.

529 The organic matter was generally higher at sites K4 and K5 and especially in higher horizons which could be
530 related to less disturbance on the topsoil and thus higher physical protection of OM in the macro-aggregates
531 (Bachmann et al., 2008). The lower OM content at least in the upper soil horizons of sites K1, K2 and K3 were
532 attributed to intense tillage (**Fig. 6a**). Moreover, K4 site where the land use included agriculture activities with
533 no tilling, has the highest carbon content. A climatic effect was not obvious for the upper 10 cm of the soils with
534 comparable clay content and different elevation like the K2 and K3 sites. On the other hand, the previous
535 argument was obvious considering the total organic carbon (kg/m³) in each site normalized to soil depth. By
536 comparing K1 and K2 sites with the terraces of K3, K4 and K5 at higher elevation (**Fig. 6b**), the lower elevation
537 sites had lower carbon accumulation compared to the higher elevation sites. However, it is difficult to attribute
538 the carbon content changes solely to a climatic effect because of the differences in land use practices between
539 the sites. The soils have been influenced by intense tilling while the different age and the different geology
540 perplex and mask the influence of other factors like climatic conditions. The millennia of anthropogenic impact

541 due to higher accessibility at the sites of lower elevation such as the fluvial areas (at least in the Roman period)
542 may have decreased substantially the carbon content.

543

544 **5 Conclusions**

545 The soil sampling in natural and manmade terraces in Koiliaris River watershed provided important insights in
546 the various processes regulating sediment provenance, soil development as well as the role of climatic variables,
547 the geomorphology, and the land uses. In general, fluvial terraces (K1 and K2) have been supplied with material
548 mainly from areas with metamorphic rocks consisted mainly of brittle texture (identical to K3 bedrock
549 lithology). Soils at terraces K3 and K4 sites developed in situ, while the K5 site showed that eolian origin
550 material and gravity transferred material from steep upland. The investigated soils have been considered to be
551 relatively young soils dating back from hundreds to several thousand years, except possibly soil at K4 site.

552 • Sites K1 and K2 were the oldest sites according to OSL dating. The K1 soil profile is the result of
553 fluvial depositional processes which was further evolved as a result of pedogenic process like calcite deposition
554 due to arid climatic conditions that prevailed for at least 1000 years. Contrary, the coarser texture of the younger
555 soil at site K2 coincided with wetter conditions.

556 • Soils at site K3 and K5 terraces were considered as young soils and no significant soil development
557 observed.

558 • K4 was developed partly from the bedrock weathering, while some plow event prior the tree plantation
559 affected probably the site, making the B horizon not discernible. Soil at K4 terrace estimated to be relatively the
560 oldest with the most extensive weathering and comparable to wet period prior soil development at sites K1 and
561 K2.

562 • The MREE and HREE depletion were readily induced in soils at K1, K2 and K3 sites, while K4 and
563 K5 sites showed to have inherited characteristics like the negative Ce^{+4} anomaly from the limestone (bedrock)
564 for the former and both from the limestone and the eolian input for the latter. Ce^{+4} positive anomaly at K1, K2
565 and K3 sites was probably controlled from other phases than Fe-Mn concretions.

566 • The organic carbon sequestration history of Crete showed that the development of manmade terraces
567 and agricultural practices without tilling increase carbon content in areas with high elevation. The intense
568 agriculture activities imposed obvious impact in the organic content at least in the upper 10 cm of the soil.

569

570 **Acknowledgments** The extensive sampling and analyses obtained in this study was financially supported from
571 the European Commission FP 7 Collaborative Project “Soil Transformations in European Catchments”
572 (SoilTrEC) (Grant Agreement no. 244118).

573

574 **References**

575 Anderson SP, Bales RC, Duff CJ (2008) Critical zone observatories: Building a network to advance
576 interdisciplinary study of Earth surface processes. *Mineral Mag* 72:7–10

577 Arianostou M (2001) Landscape changes in Mediterranean ecosystems of Greece: implications for fire and
578 biodiversity issues. *J Mediterr Ecol* 2:165-178

579 Aubert D, Stille P, Probst A, (2001) REE fractionation during granite weathering and removal by waters and
580 suspended loads: Sr and Nd isotopic evidence. *Geochim. Cosmochim. Acta* 65: 387– 406

- 581 Bachmann J, Guggenberger G, Baumgartl T, Ellerbrock R.H, Urbanek E, Goebel M.-O, Kaiser K, Horn R,
582 Fischer WR (2008) Physical carbon-sequestration mechanisms under special consideration of soil
583 wettability. *J Plant Nutr Soil Sc* 171:14-26
- 584 Banwart S (2011) Save Our Soils. *Nature* 474:152-151
- 585 Barea JM, Pozo MJ, Azcon R, Azcon-Aguilar C (2005) Microbial co-operation in the rhizosphere. *J Exper Bot*
586 56:1761–1778
- 587 Baumann A, Best G, Swosdz W, Wachendorf H (1976) The nappe pile of eastern Crete. *Tectonophysics*
588 30:T33-T40
- 589 Bayon G, Dennielou B, Etoubleau J, Ponzevera E, Toucanne S, Bermell S (2012) Intensifying Weathering and
590 Land Use in Iron Age Central Africa. *Science* 335:1219-1222
- 591 Brantley SL, Goldhaber MB, and Ragnarsdottir KV (2007) Crossing disciplines and scales to understand the
592 Critical Zone. *Elements* 3:307-314
- 593 Bronick CJ, Lal R (2005) Soil structure and management: a review. *Geoderma* 124:3-22
- 594 Casana J (2008) Mediterranean valleys revisited: Linking soil erosion, land use and climate variability in the
595 Northern Levant. *Geomorphology* 101:429-442
- 596 Charitopoulos E, Sarris A (2009) Documenting Venetian and Ottoman landscape in Crete: Settlement patterns,
597 road network and productive areas in Rethymnon inland 14th International Congress “Cultural Heritage
598 and New Technologies” Vienna
- 599 Compton JS, White RA, Smith M (2003) Rare earth element behavior in soils and salt pan sediments of a semi-
600 arid granitic terrain in the Western Cape, South Africa. *Chem Geol* 201:239-255
- 601 Coppin F, Berger G, Bauer A, Castet S, Loubet M (2002) Sorption of lanthanides on smectite and kaolinite.
602 *Chem Geol* 182:57–68
- 603 Davidovich U, Porat N, Gadot Y, Avni Y, Lipschits O (2012) Archaeological investigations and OSL dating of
604 terraces at Ramat Rahel, Israel. *J Field Archaeol* 37:192-208
- 605 Dornsiepen UF, Manutsoglu E, Mertmann D (2001) Permian-Triassic palaeogeography of the external
606 Hellenides. *Palaeogeogr Palaeoclimatol* 172:327-338
- 607 Dotterweich M (2013) The history of human-induced soil erosion: Geomorphic legacies, early descriptions and
608 research, and the development of soil conservation—A global synopsis. *Geomorphology* 201:1-34
- 609 Eger A, Almond PC, Condon LM (2011) Pedogenesis, soil mass balance, phosphorus dynamics and vegetation
610 communities across a Holocene soil chronosequence in a super-humid climate, South Westland, New
611 Zealand. *Geoderma* 163:185-196
- 612 Elderfield H, Greaves MJ (1982) The rare earth elements distribution in seawater. *Nature* 296: 214–219
- 613 FAO (2006) World reference base for soil resources, World Soil Resources Reports No. 1032nd edition. Food
614 and agriculture organization of the United Nations, FAO, Rome
- 615 Fedoroff N (1997) Clay illuviation in Red Mediterranean soils. *Catena* 28:171-189
- 616 Francke A, Wagner B, Leng M J, Rethemeyer J (2012) A Late Glacial to Holocene record of environmental
617 change from LakeDojran (Macedonia, Greece) *Clim Past Discuss* 8:5743–5785

- 618 Gromet LP, Dymek RF, Haskin LA, Korotev RL (1984) The “North American shale composite”: Its
619 compilation, major and trace element characteristics. *Geochim Cosmochim Acta* 48:2469-2482
- 620 Grove AT, Rackham O (1993) Threatened landscapes in the Mediterranean: examples from Crete. *Landscape*
621 *Urban Plan* 24:279–292
- 622 Imai N, Terashima S, Itoh S, Ando A (1998) Compilation of analytical data for five GSJ geochemical reference
623 samples: the “Instrumental Analysis Series”. *Geostandard Newslett* 23:223–250
- 624 Johannesson KH, Zhou X, Guo C, Stetzenbach KJ and Hodge VF (2000) Origin of rare earth element signatures
625 in groundwaters of circumneutral pH from southern Nevada and eastern California, USA. *Chem Geol*
626 164:239–257
- 627 Kalderon-Asael B, Erel Y, Sandler A, Dayan U (2009) Mineralogical and chemical characterization of
628 suspended atmospheric particles over the east Mediterranean based on synoptic-scale circulation patterns.
629 *Atmos Environ* 43:3963-3970
- 630 Kéfi S, Rietkerk M, Alados CL, Pueyo Y, Papanastasis VP, ElAich A, Ruitter PC (2007) Spatial vegetation
631 patterns and imminent desertification in Mediterranean arid ecosystems. *Nature* 449:213–217
- 632 Kizos T, Koulouri M (2006) Agricultural landscape dynamics in the Mediterranean: Lesvos (Greece) case study
633 using evidence from the last three centuries. *Environ Sci Policy* 9:330-342
- 634 Kourgialas NN, Karatzas GP, Nikolaidis NP (2010) An integrated framework for the hydrologic simulation of a
635 complex geomorphological river basin. *J Hydrol* 381:308-321
- 636 Kourgialas NN, Karatzas GP, Nikolaidis NP (2011) Development of a thresholds approach for real-time flash
637 flood prediction in complex geomorphological river basins. *Hydrol. Process* DOI: 10.1002/hyp.8272
- 638 Lair GJ, Zehetner F, Hrachowitz M, Franz N, Maringer FJ, Gerzabek MH (2009) Dating of soil layers in a
639 young floodplain using iron oxide crystallinity. *Quaternary Geochronology* 4:260-266
- 640 Laveuf C, Cornu S (2009) A review on the potentiality of Rare Earth Elements to trace pedogenetic processes.
641 *Geoderma* 154:1-12
- 642 Laveuf C, Cornu S, Guilherme LRG, Guerin A, Juillot F (2012) The impact of redox conditions on the rare earth
643 element signature of redoximorphic features in a soil sequence developed from limestone. *Geoderma*
644 170:25-38
- 645 Laveuf C, Cornu S, Juillot F (2008) Rare earth elements as tracers of pedogenic processes. *C. R. Geoscience*
646 340: 523-532
- 647 Le Roy EL (1971). *Times of Feast, Times of Famine: a History of Climate Since the Year 1000*. Barbara Bray.
648 Garden City, NY: Doubleday
- 649 Leybourne MI, Johannesson KH (2008) Rare earth elements (REE) and yttrium in stream waters, stream
650 sediments, and Fe-Mn oxyhydroxides: Fractionation, speciation, and controls over REE + Y patterns in
651 the surface environment. *Geochim Cosmochim Acta* 72:5962-5983
- 652 Lomax J, Fuchs M, Preusser F, Fiebig M (2012) Luminescence based loess chronostratigraphy of the Upper
653 Palaeolithic site Krems-Wachtberg, Austria. *Quatern Int* (in press)

- 654 Long-Jiang M, Duo-Wen M, Jing-Hong Y, Chen-Xi S (2009) Geochemistry of trace and rare earth elements in
655 red soils from the Dongting lake area and its environmental significance. *Pedosphere* 19:615-622
- 656 Ma Y-J., Huo R-K, Liu, C-Q (2002) Speciation and fractionation of rare earth elements in a lateritic profile
657 from southern China: identification of the carriers of Ce anomalies. *Proceedings of the Goldschmidt*
658 *Conference, Davos, Switzerland.*
- 659 Macklin MG, Tooth S, Brewer PA, Noble PL, Duller GAT (2010) Holocene flooding and river development in
660 a Mediterranean steep-land catchment: The Anapodaris Gorge, south central Crete, Greece. *Global Planet*
661 *Change* 70:35-52
- 662 Marini JC, Chauvel C, Maury RC (2005) Hf isotope compositions of northern Luzon arc lavas suggest
663 involvement of pelagic sediments in their source. *Contrib Mineral Petrol* 149:216–232
- 664 McLennan SM (1989) Rare earth elements in sedimentary rocks: influence of provenance and sedimentary
665 processes. In: Lipin BR and McKay, GA, (eds) *Geochemistry and Mineralogy of Rare Earth Elements.*
666 *Rev Mineral* 21:169–200
- 667 Miao L, Xu R, Ma Y, Zhu Z, Wang J, Cai R, Chen Y, (2008) Geochemistry and biogeochemistry of rare earth
668 elements in a surface environment (soil and plant) in South China. *Environ Geol* 56:225–235
- 669 Millennium Ecosystem Assessment (MEA) (2005) *Ecosystems and Human Well-being: Synthesis.* Island Press,
670 Washington, DC
- 671 Montgomery DJ (2010) 2020 Visions. *Nature* 463: 26-32
- 672 Moraetis D, Efstathiou D, Stamati FE, Tzoraki O, Nikolaidis NP, Schnoor JL, Vozinakis K (2010) High-
673 frequency monitoring for the identification of hydrological and bio-geochemical processes in a
674 Mediterranean river basin. *J Hydrol* 389:127-136
- 675 Mouslopoulou V, Moraetis D, Fassoulas C (2011) Identifying past earthquakes on carbonate faults: Advances
676 and limitations of the ‘Rare Earth Element’ method based on analysis of the Spili Fault, Crete, Greece.
677 *Earth Planet Sci Lett* 309:45-55
- 678 Muhs DR, Budahn J, Avila A, Skipp G, Freeman J, Patterson de A (2010) The role of African dust in the
679 formation of Quaternary soils on Mallorca, Spain and implications for the genesis of Red Mediterranean
680 soils. *Quaternary Sci Rev* 29:2518-2543
- 681 Murray RW, Buchholtz MR, Brink T, Brumsack HJ, Gerlach DC, Russ GP (1991b) Rare earth elements in
682 Japan Sea sediments and diagenetic behavior of Ce/Ce*: Results from ODP Leg 127. *Geochim*
683 *Cosmochim Acta* 55:2453-2466
- 684 Nihlén T, Mattsson OJ, Rapp A, Gagaoudaki C, Kornaros G, Papageorgiou J (1995) Monitoring of Sahara dust
685 fallout on Crete and its contribution to soil formation. *Tellus* 47B: 365-374
- 686 Papanikolaou D, Vassilakis E (2010) Thrust faults and extensional detachment faults in Cretan tectono-
687 stratigraphy: Implications for Middle Miocene extension. *Tectonophysics* 488:233–247
- 688 Pope R, Wilkinson K, Skourtsos E, Triantaphyllou M, Ferrier G (2008) Clarifying stages of alluvium fan
689 evolution along the Sfakian piedmont, southern Crete: New evidence from analysis of post-incisive soils
690 and OSL dating. *Geomorphology* 94:206-225

- 691 Raymond PA, Cole JJ (2003) Increase in the export of alkalinity from North America's largest river. *Science*
692 301:88-91
- 693 Sarah P (2005) Soil aggregation response to long- and short-term differences in rainfall amount under arid and
694 Mediterranean climate conditions. *Geomorphology* 70:1-11
- 695 Scarciglia F, Tuccimei P, Andrea Vacca A, Barca D, Pulice I, Salzano R, Soligo M (2011) Soil genesis,
696 morphodynamic processes and chronological implications in two soil transects of SE Sardinia, Italy:
697 Traditional pedological study coupled with laser ablation ICP-MS and radionuclide analyses. *Quatern Int*
698 233:40-52
- 699 Sholkovitz ER, Schneider DL (1991) Cerium redox cycles and rare earth elements in the Sargasso Sea. *Geochim*
700 *Cosmochim Ac* 55:2737–2743
- 701 Siart C, Hecht S, Holzhauser I, Altherr R, Meyer HP, Schukraft G, Eitel B, Bubenzer O, Panagiotopoulos D
702 (2010) Karst depressions as geoarchaeological archives: the palaeoenvironmental reconstruction of
703 Zominthos (Central Crete) based on geophysical prospection, mineralogical investigations and GIS.
704 *Quatern Int* 216:75-92
- 705 Six J, Bossuyt H, Degryze S, Denef K (2004a) A history of research on the link between (micro)aggregates, soil
706 biota, and soil organic matter dynamics. *Soil Till Res* 79:7–31
- 707 Six J, Conant RT, Paul EA, Paustian K (2002) Stabilization mechanisms of soil organic matter: Implications for
708 C-saturation of soils. *Plant Soil* 241:155-176
- 709 Six J, Elliott ET, Paustian K (2000a) Soil macroaggregate turnover and microaggregate formation: a mechanism
710 for C sequestration under no-tillage agriculture. *Soil Biol Biochem* 32:2099-2103
- 711 Soil Survey Staff (2004) Soil Survey Laboratory Methods Manual. Soil Survey Investigations Rep. 42. USDA –
712 NRCS, Washington, DC
- 713 Stamati FE, Nikolaidis NP, Venieri D, Psillakis E, Kalogerakis N (2011) Dissolved organic nitrogen as an
714 indicator of livestock impacts on soil biochemical quality. *Appl Geochem* 26: S340-S343
- 715 Solleiro-Rebolledo E, Sycheva S, Sedov S, McClung de Tapia E, Rivera-Uria Y, Salcido-Berkovich C,
716 Kuznetsova A (2011) Fluvial processes and paleopedogenesis in the Teotihuacan Valley, México:
717 Responses to late Quaternary environmental changes. *Quatern Int* 233:40-52
- 718 Stallsmith BA (2007) One colony, Two mother cities: Cretan Agriculture under Venetian and Ottoman Rule,
719 JSTOR
- 720 Thomas CW (1993) Sources of rare earth elements in Appin Group limestones, Dalradian, north east Scotland.
721 *Miner Petrol* 49:27-44
- 722 UNEP (2012) Emerging issues in our global environment . UNOP Nairobi, ISO 10041:2004, 19-31
- 723 Wagner B, Lotter AF, Nowaczyk N, Reed, JM, Schwalb A, Sulpizio R, Valsecchi V, Wessels, M, Zanchetta G
724 (2009) A 40,000-year record of environmental change from ancient Lake Ohrid (Albania and Macedonia).
725 *J Paleolimnol* 41:407–430
- 726 Wan Y, Liu C (2005) Study on Adsorption of Rare Earth Elements by Kaolinite. *J Rare Earth* 23:377-381
- 727 Wu G, Zhang X, Zhang C, Gao S, Li Z, Wang F, Wang W (2010) Concentration and composition of dust
728 particles in surface snow at Urumqi Glacier, No. 1, Eastern Tien Shan. *Global Planet Change* 74: 34–42

- 729 Xing B, Dudas MJ (1993) Trace and rare earth element content of white clay soils of the Three River Plain,
730 Heilongjiang Province, P. R. China. *Geoderma* 58:181–199
- 731 Zacharias N, Bassiakos Y, Hayden B, Theodorakopoulos K, Michael CT (2009) Luminescence dating of deltaic
732 deposits from eastern Crete, Greece. *Geoarcheological implications. Geomorphology* 109:46-53
- 733 Zhaoliang S, Congqiang L, Guilin H, Zhongliang W, Zhaoshou Z, Cheng Y (2006) Enrichment and release of
734 rare earth elements during weathering of sedimentary rocks in Wujiang Catchments, SW China. *J*
735 *Rare Earth* 24:491-496
- 736
- 737
- 738

739
740
741
742
743
744
745

Table 1 Physical and chemical characteristics of the identified soil horizons at the 5 different sites K1, K2, K3, K4, K5.

Site	Horizon	Depth (cm)	EC	pH	stdev	Organic C (g/kg)	stdev	CaCO ₃ (g/kg)	stdev	Bulk density (g/cm ³)	stdev	Texture	Clay (%)	stdev	OSL dating (depth: m/years)	
K1	Apk	0-5	317	7.7	-	15.2	-	41.3	-	1.47	-	si l	15.1	-	0.85/ 2400 (±400)	
	Apk	5-10		7.8	0.2	14.8	0.5	44.0	33.7	1.38	0.02	si l	16.9	1.5		
	ACk	29-34	296	7.9	0.1	7.6	1.3	74.0	41.9	1.48	0.05	si l	20.2	1.3		
	C1k	45-50	-	8.1	0.1	4.6	0.3	133.8	23.2	1.60	0.02	si l	20.7	1.6		
	C2k	72-77	-	8.1	-	4.3	-	117.3	-	-	-	si l	19.9	-		
	C3k	95-100	-	8.1	-	2.9	-	107.7	-	1.66	-	l	18.9	-		
K2	ACp	0-5	150	6.5	0.8	19.0	3.3	22.7	19.3	1.24	0.04	sa l	5.5	0.2	0.45/1400 (±400)	
	C1k	5-10		6.0	1.1	16.7	2.2	21.8	17.1	1.25	0.04	sa l	4.7	0.7		
	C2k	55-60		93	5.9	1.3	4.8	1.1	16.6	13.1	1.38	0.03	sa l	5.2		1.1
K3	ACp	0-5	93	6.0	-	15.8	-	2.2	-	1.34	0.05	sa l	6.8	-		
	ACp	5-10	58	5.9	1.0	18.4	1.2	11.4	16.1	1.27	0.1	sa l	5.8	1.9		
	CR	20-27	-	7.4	-	18.3	-	29.8	-	-	-	sa l	6.4	-		
K4	Ah	0-5	167	5.7	0.5	71.8	16.5	2.2	0.5	1.10	-	si cl l	24.1	10.4		
	AC	5-10		4.9	0.4	37.7	1.9	1.3	0.7	-	-	si cl l	29.1	10.6		
	C1	15-50		73	4.3	0.1	18.1	3.7	0.7	0.3	-	-	si cl l	35.9		15.6
	C2	50-60		-	4.7	-	5.2	-	1.0	-	-	-	si cl	48.5		-
K5	Ah	0-5	96	6.0	0.1	42.8	6.7	1.6	0.3	1.06	0.07	si cl l	24.3	9.6	0.45/580 (±120)	
	AC1	7-12		5.8	0.1	22.7	0.9	0.9	0.02	1.21	0.07	si cl l	25.3	8.4		
	AC2	40-45		75	6.0	0.2	22.6	2.5	0.8	0.6	1.07	0.05	si cl l	27.1		9.4
	AC3	60-90		-	6.1	-	16.5	-	0.4	-	-	-	si cl l	34.6		-

746
747
748
749
750
751
752

stdev: Standard deviation derived from the three pits of each site
 EC: electrical conductivity measured for 0-10 cm and a lower horizon
 si l: silty loam, sa l: sandy loam, l: loam, si cl: silty clay, sic l l: silty clay loam
 -: not measured

753
754
755
756

Table 2 Chemical analysis in 2mm soil fraction in two different soil horizons at each site (w/w %).

Site	Horizon	Sampling depth cm	Na ₂ O	MgO	K ₂ O	CaO	TiO ₂	MnO	Fe ₂ O ₃	Al ₂ O ₃	SiO ₂	P ₂ O ₅	LOI
K1	Apk	0-10	1.3	2.2	1.7	3.4	0.9	0.1	6.5	13.6	61.4	0.2	10.2
	ACk	29-34	1.5	2.2	1.6	3.5	0.9	0.1	6.3	13.9	59.3	0.2	10.0
K2	ACpk/ C1k	0-10	1.3	1.6	1.5	2.9	0.8	0.1	5.6	11.3	67.5	0.2	7.4
	C2k	55-60	1.3	1.2	1.3	2.2	0.7	0.1	5.2	10.4	71.3	0.2	4.4
K3	ACp	0-10	1.5	1.3	2.5	0.4	1.0	0.1	8.8	19.3	58.1	0.1	8.8
	CR	20-27	1.7	1.2	2.5	0.3	1.0	0.1	8.8	19.4	57.8	0.1	7.1
K4	Ah/AC	0-10	-	0.9	1.1	0.6	0.4	-	4.8	8.9	75.0	0.3	9.0
	C1	15-20	0.8	0.9	1.1	0.3	0.4	-	5.3	10.4	72.3	0.3	9.2
K5	Ah/AC1	0-12	-	4.0	2.8	0.8	0.9	0.5	9.5	16.6	52.5	0.3	12.0
	AC2	40-45	0.5	4.8	3.1	0.9	0.9	0.6	9.8	17.4	49.5	0.3	12.8

-: Na₂O <0.3%, MnO<0.01

LOI: Loss of ignition

757
758
759
760
761
762
763
764
765
766
767
768
769
770
771
772
773
774
775
776
777
778

779
780
781

Table 3 Chemical analysis in 2µm fraction in all soil horizons at each site(w/w %).

Site	Horizon	Sampling depth cm	Na ₂ O	MgO	K ₂ O	CaO	TiO ₂	MnO	Fe ₂ O ₃	Al ₂ O ₃	SiO ₂	P ₂ O ₅	LOI
K1	Apk	0-10	-	2.6	2.3	4.1	1.2	0.2	8.8	17.0	34.5	0.5	28.9
	ACk	29-34	-	2.9	2.6	3.0	1.3	0.2	9.4	18.8	38.4	0.6	22.8
	C1k	45-50	-	-	2.5	6.5	1.3	0.2	9.9	18.7	35.3	0.7	25.0
	C2k	72-77	-	2.7	2.1	6.8	1.2	0.2	10.6	17.5	36.6	0.5	21.6
K2	Ack/C1k	0-10	-	-	2.4	1.0	1.1	0.2	8.1	16.7	33.3	0.5	36.4
	C2k	55-60	-	-	2.2	1.2	1.1	0.2	8.1	15.4	44.2	-	27.1
K3	ACp	0-10	-	-	3.0	0.5	1.7	0.2	10.9	21.4	35.3	0.5	26.5
	CR	20-27	-	-	3.0	0.4	1.9	0.2	11.6	21.9	35.7	-	25.3
K4	Ah/AC	0-10	-	2.8	2.0	0.7	1.1	0.1	9.0	21.5	38.9	0.8	23.2
	C1	15-20	-	3.2	2.1	0.4	1.2	-	8.8	21.3	42.2	0.7	20.1
	C2	50-60	-	3.3	2.0	0.5	1.2	0.1	9.3	23.2	41.5	0.5	18.3
K5	Ah/AC1	0-12	-	5.3	3.3	0.7	1.3	0.7	8.1	21.1	39.5	0.6	19.4
	AC2	40-45	-	5.2	3.3	0.9	1.3	0.6	8.3	21.2	40.3	0.6	18.3
	AC3	60-90	-	4.8	3.1	0.8	1.3	0.6	8.6	21.8	40.5	0.6	17.9

782 -: Na₂O <0.5%, MgO<0.2%, MnO<0.01, P₂O₅<0.05%

783 Standard error: P₂O₅: 0.01, TiO₂: 0.01, Al₂O₃:0.1, K₂O: 0.07, SiO₂: 0.01, Na₂O: 0.05 Fe₂O₃: 0.01, CaO: 0.05

784
785
786
787
788
789
790
791
792

793

Table 4 Quantitative mineralogical analysis (percentage) in all sites at different depths in the soil profile (depth in parentheses in cm).

<2mm	K1 (0-10)	K1 (29-34)	K2 (0-10)	K2 (55-60)	K3 (0-10)	K3 (20-27)	K4 (0-10)	K4 (15-20)	K5 (0-12)	K5 (40-45)
Calcite	1	6	2	3	-	-	-	-	-	-
Chlorite	-	-	-	-	-	-	-	-	11	12
Dolomite	-	-	4	2	-	-	-	-	-	-
Feldspars	4	7	5	3	6	6	3	2	9	11
Hematite	-	-	-	-	-	-	0.2	1	-	1
Illite	3	3	4	1	2	2	17	27	41	28
Kaolinite	11	14	8	12	13	15	23	19	11	14
Muscovite	13	10	14	10	19	1	7	5	0.3	14
Paragonite	10	trace	3	7	12	36	-	-	-	-
Phillipsite	6	6	6	8	-	-	-	-	-	-
Quartz	52	53	54	53	48	40	50	46	28	19
Vermiculite	<1	<1	<1	<1	<1	traces	-	traces	-	-

<2µm	K1 (0-10)	K1 (29-34)	K1 (45-50)	K1 (72-77)	K2 (0-10)	K2 (55-60)	K3 (0-10)	K3 (10-27)	K4 (0-10)	K4 (15-20)	K4 (55-60)	K5 (0-10)	K5 (40-45)	K5 (75-90)
Calcite	1	2	9	8	-	-	-	-	-	-	-	-	-	-
Chlorite	-	-	-	-	-	-	-	-	-	-	-	9	9	7
Dolomite	-	-	-	-	-	2	-	-	-	-	-	-	-	-
illite	39	53	39	32	37	36	36	29	34	38	38	37	48	42
Feldspars	5	-	3	4	4	6	10	10	1	-	-	5	3	3
He/Goe	2	-	2	4	2	1	5	5	5	4	4	2	3	4
Kaolinite	13	20	11	19	21	22	27	25	33	37	37	17	19	14
Muscovite	32	18	29	26	17	3	10	23	22	16	15	28	15	25
Paragonite	3	-	2	3	5	7	3	2	-	-	-	-	-	-
Phillipsite	-	-	-	-	5	8	-	-	-	-	-	-	-	-
Quartz	4	5	4	3	8	15	6	6	4	5	5	2	4	3
Vermiculite	<1	1	<1	<1	<1	<1	<1	traces	traces	traces	traces			

794

-: not presented

795

Traces: mineral peak was identified but quantification was not possible

796 **Fig. 1** Geology map of the Koiliaris CZO, with the tributaries of Koiliaris river (1,2,3), the sampling sites (K1,
797 K2, K3, K4, K5) and the Stylos karstic spring.

798

799 **Fig. 2** Schematic diagram of the geomorphology of the sites K1-K5 according to their elevation, soil profile and
800 horizon characterization. The gray color bands show the sampled horizons. Current land use was also depicted.

801

802 **Fig. 3** a) PCA for physical and chemical parameters for the main soil profiles in each site for all identified
803 horizons considering PSD, calcite content, organic content and pH, b) PCA for the trace metals content (Li, B,
804 Ti, Cr, Mn, Ni, Cu, Zn, As, Rb, Sr, Y, Cs, Ba, Pb, U, Zr, Nb) for two horizons and one or two replicates in each
805 site. The upper horizons (0-10 cm) denoted with u, the lower horizons were not ascribed with symbol.
806 Replicates were also presented (rep)

807

808 **Fig. 4** Rare earth elements concentration normalized to NASC (Gromet et al. 1984) for two soil horizons and the
809 corresponding parent materials in a) K1-K3 sites (parent material only from K3 site is presented: metamorphic
810 rocks), b) K4-K5 sites and the corresponding parent materials (three different lithologies presented for K5 site).
811 Two replicates (rep.) were presented.

812

813 **Fig. 5** a) OSL results in the Koiliaris CZO, and climatic variability identified it two areas in Greece, lake Doiran
814 in northern Greece (Francke et al. 2012) and the Anapodaris river in Crete for late Holocene (Macklin et al.
815 2010).

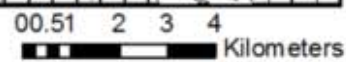
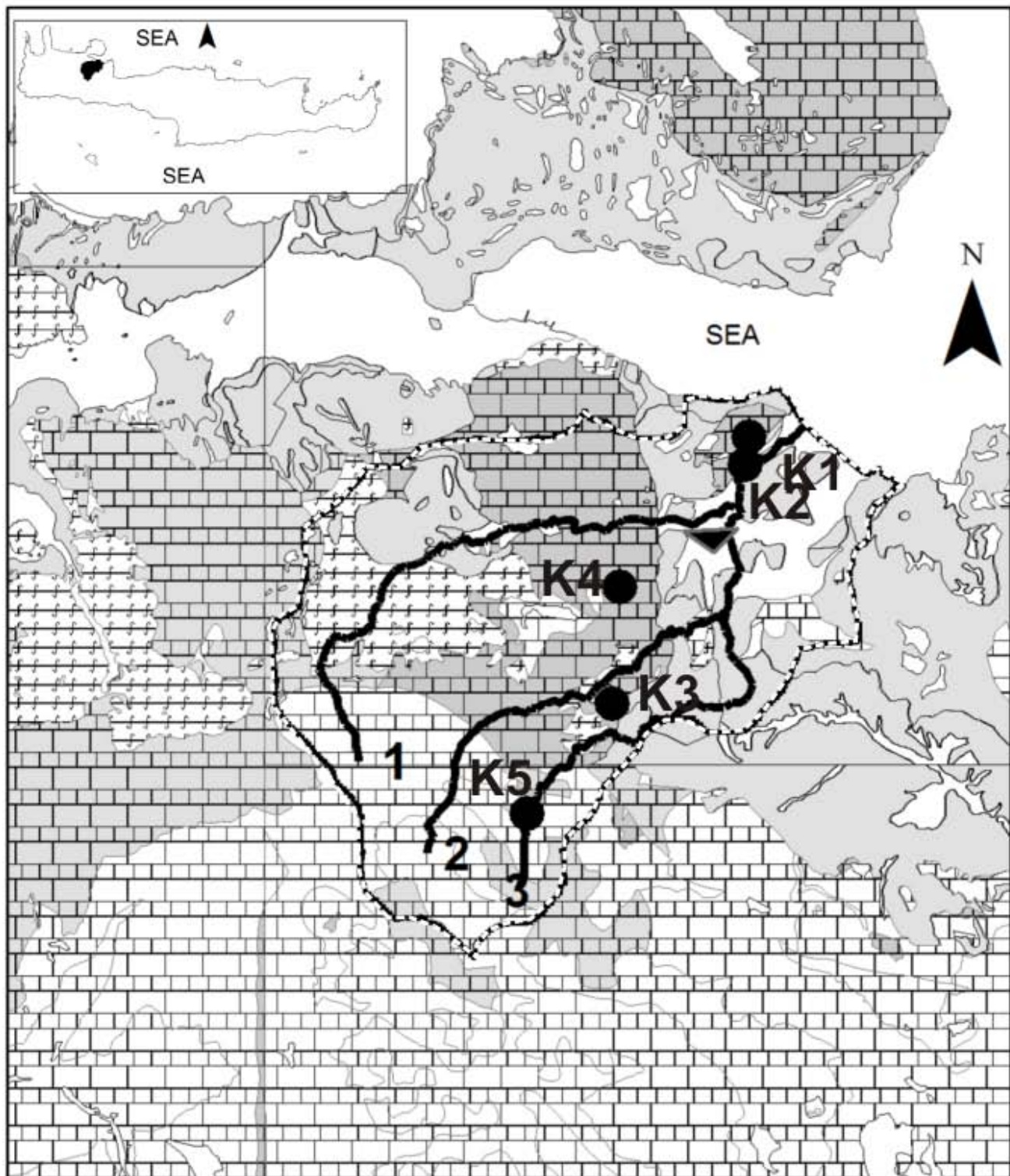
816

817 **Fig. 6** a) Organic carbon (kg/m^3) in the upper soil horizons (0-12 cm) at each site b) Total organic carbon kg/m^3
818 at each site. All values were normalised to soil depth.

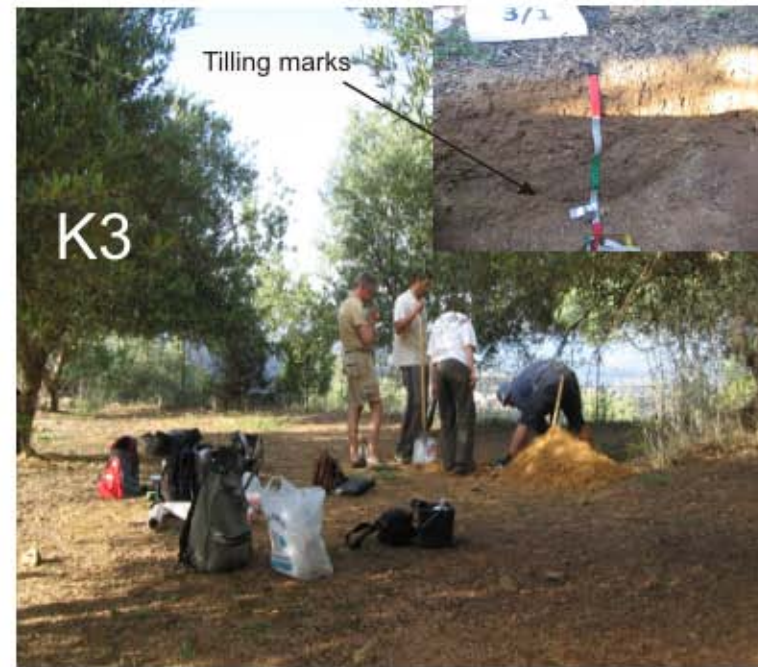
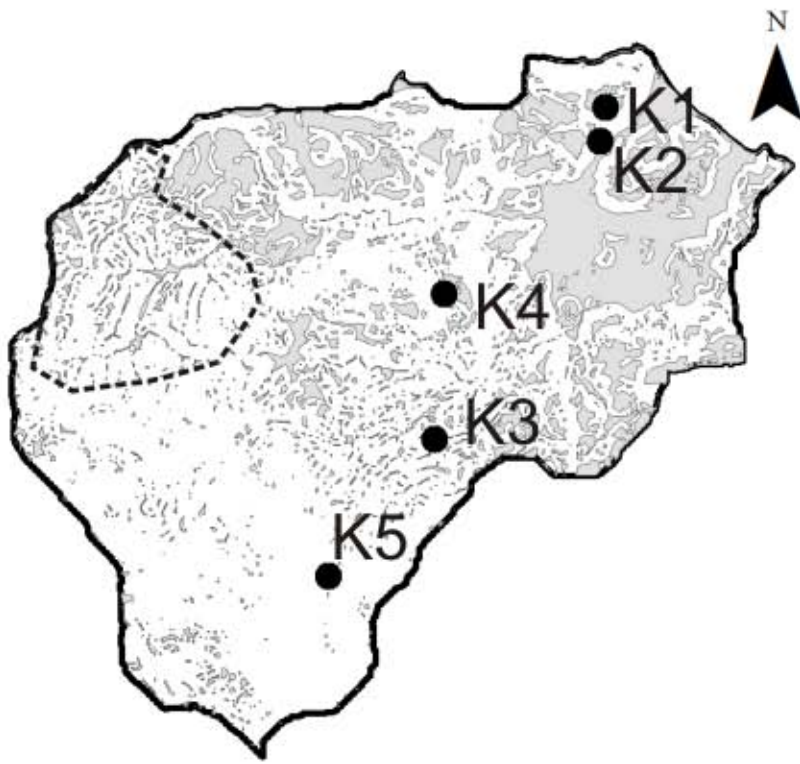
819

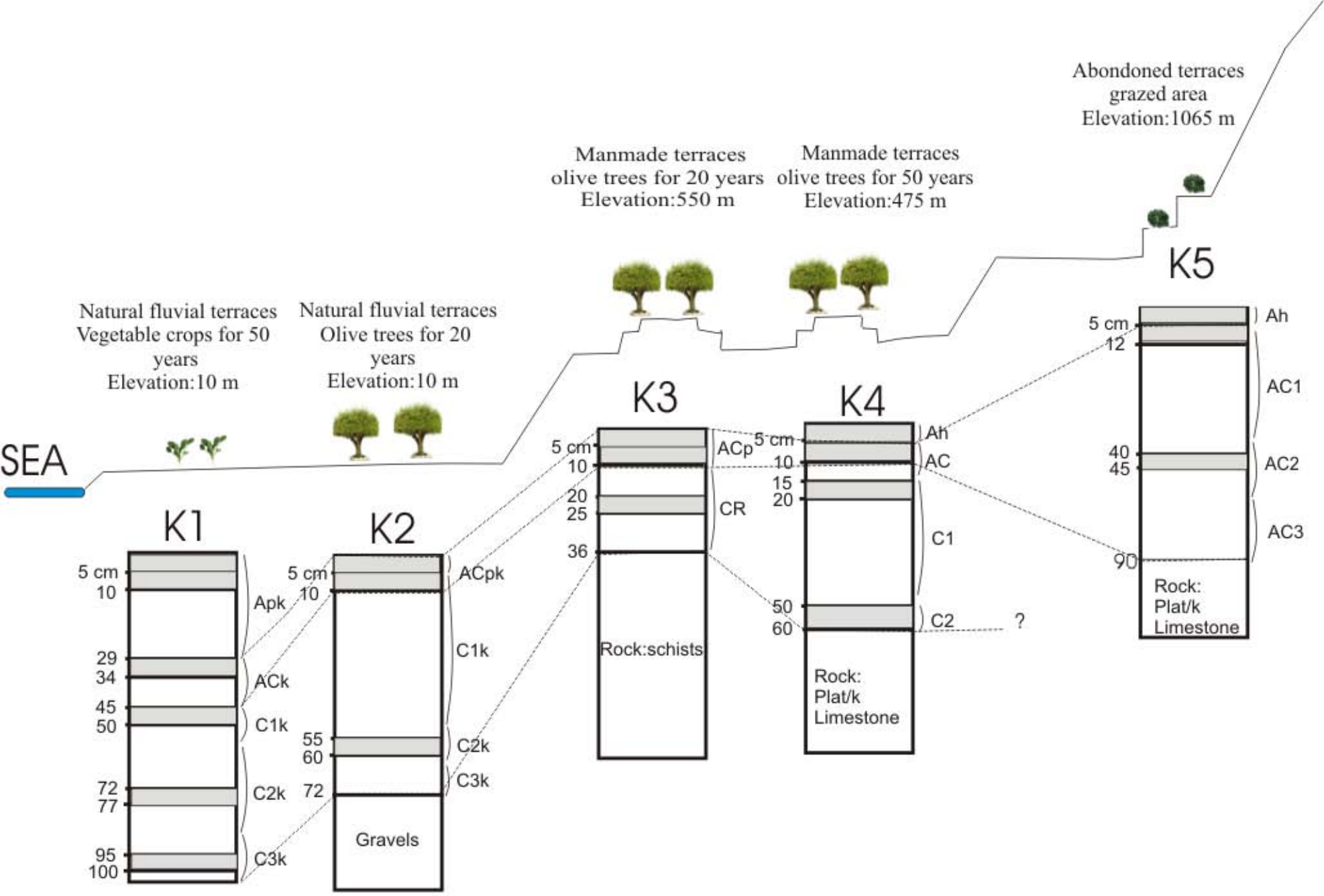
820

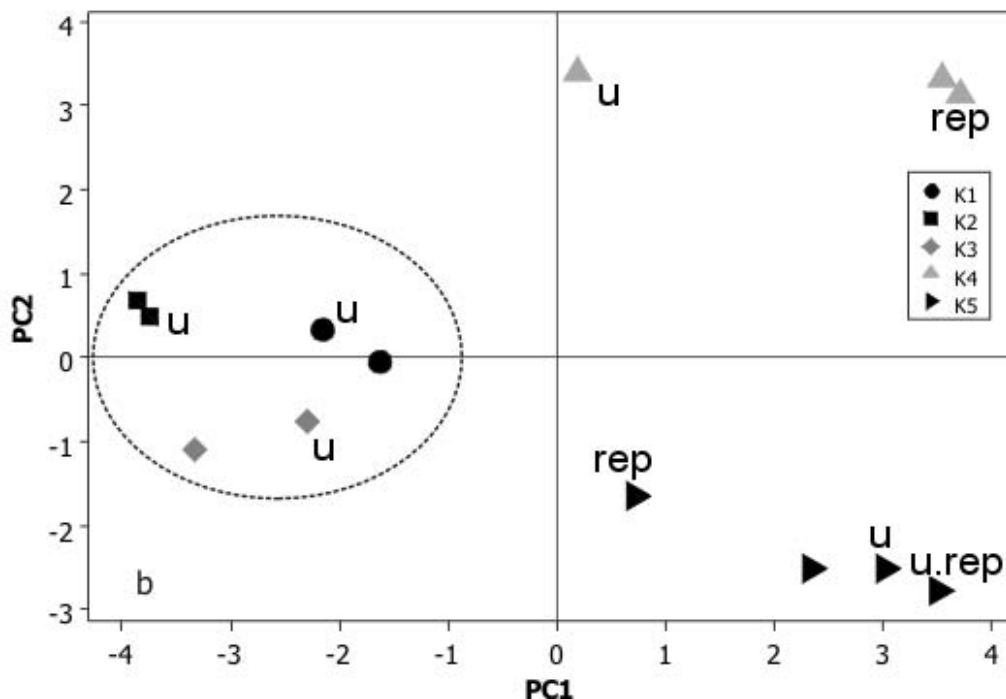
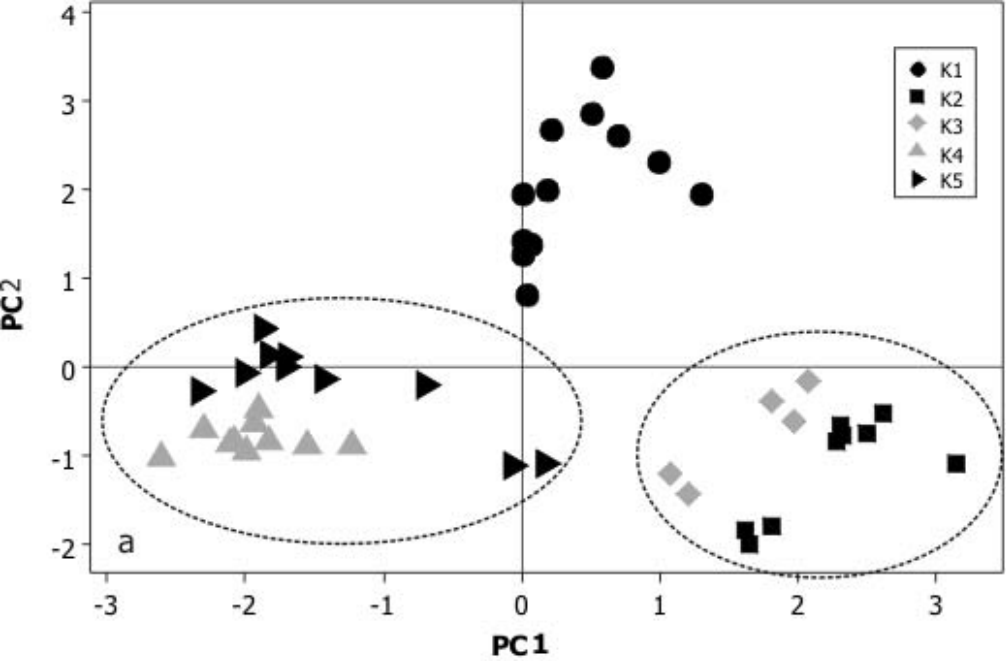
821

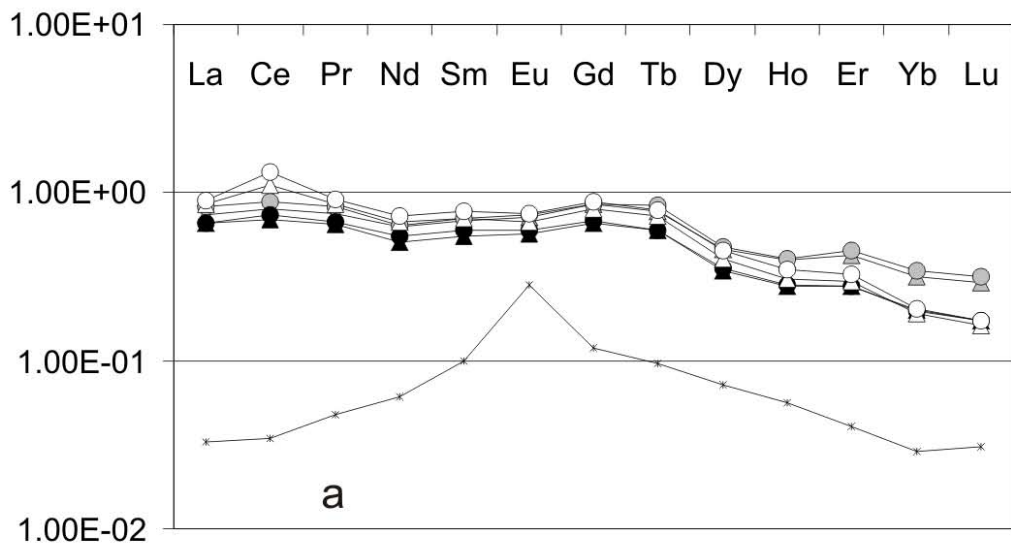


- | | |
|---|-------------------------|
| Alluvium | Rivers |
| Neogene marls and marly limestones | 1 Keriamianos tributary |
| Metamorphic schists | 2 Milavlakas tributary |
| Trypali nappe limestones | 3 Mantamas tributary |
| Plattenkalk nappe- limestones-dolomites with cherts | watershed |
| | Stylos spring |
| | Sampling sites |

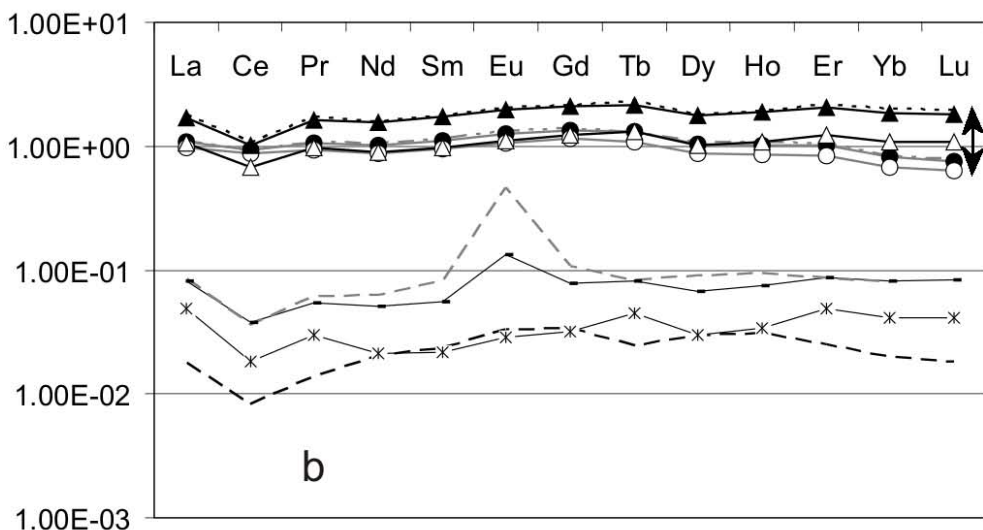








- ▲ K1-Apk 0-10 cm
- ▲ K2-ACpk 0-10 cm
- △ K3 ACp 0-10 cm
- * Ph/Qu-K3 (schists)
- K1-ACk 29-34 cm
- K2-C2k 55-60 cm
- K3-CR 20-25cm



- K5-AC2 40-45 cm
- K5-Ah/AC1 0-12 cm
- ⋯ K4-C1 (rep)
- * Plattenkalk-K5 (lim/ne)
- - Plattenkalk-K5 (chert)
- - K5-AC2 (rep)
- ▲ K4-C1 15-20 cm
- △ K4-Ah/AC 0-10 cm
- Plattenkalk-K5 (lim/ne_bitumen)
- - Plattenkalk-K4 (lim/ne)

